

Electronic Supplementary Material

Ultrastable, Stretchable, High-conductive and Transparent Hydrogels Enabled by Salt-Percolation for High-performance Temperature and Strain Sensing

Zixuan Wu¹, Wenxiong Shi², Haojun Ding¹, Bizhang Zhong¹, Wenxi Huang¹, Yubin Zhou³, Xuchun Gui¹, Xi Xie¹, and Jin Wu^{1*}

¹State Key Laboratory of Optoelectronic Materials and Technologies and the Guangdong Province Key Laboratory of Display Material and Technology, School of Electronics and Information Technology, Sun Yat-sen University, Guangzhou 510275, China

²Institute for New Energy Materials and Low Carbon Technologies, School of Materials Science and Engineering, Tianjin University of Technology, Tianjin 300384, China

³School of Pharmacy, Guangdong Medical University, Dongguan 523808, P. R. China

*Correspondence should be addressed to J. W. (Email: wujin8@mail.sysu.edu.cn)

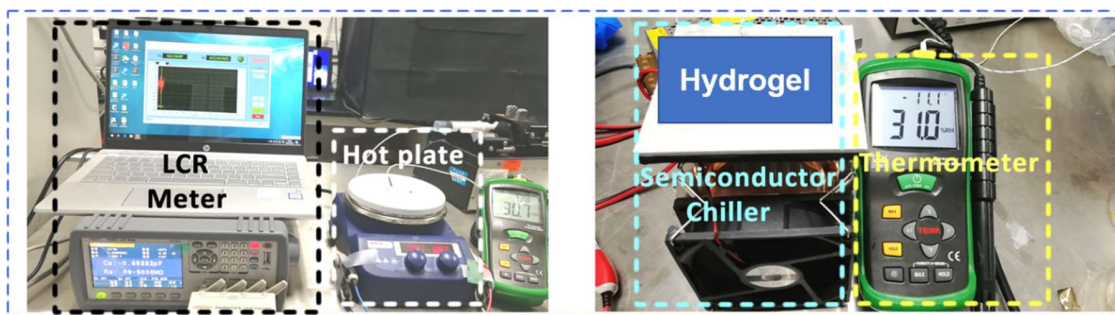


Figure S1. Experimental setup of temperature sensing when heating (left) and cooling (right) were performed.

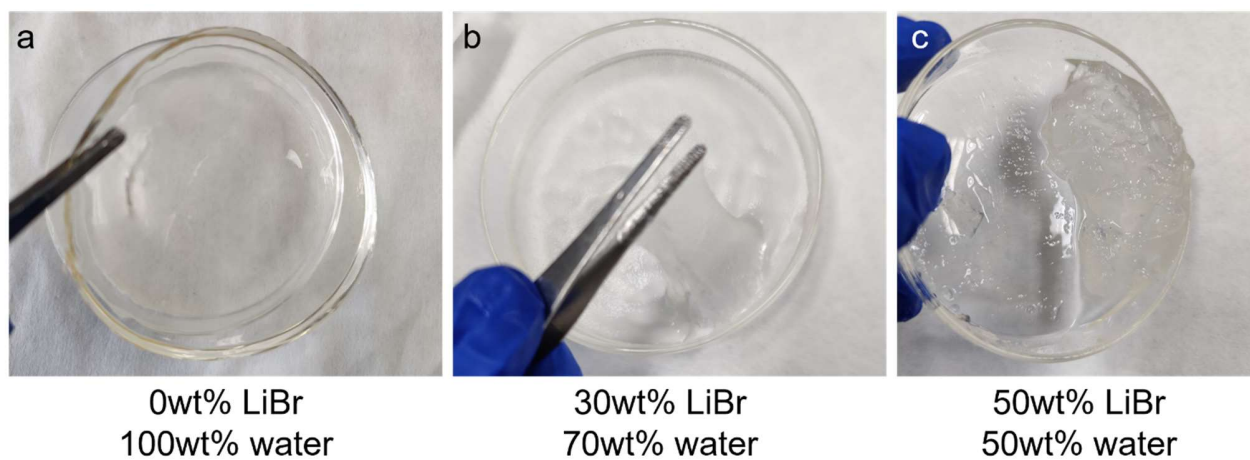


Figure S2. Photographs of samples obtained by adding LiBr with different concentrations in the pre-gel precursor solution for polymerization: a) 100wt% deionized (DI) water; b) 30wt% LiBr, 70wt% DI water; c) 50wt%LiBr, 50wt% DI water. It was clear that the AAm/carrageenan polymerized in (a), partially polymerized in (b), and did not polymerize in (c), respectively. This demonstrates that the addition of salts such as LiBr in the precursor solution impedes the polymerization of AAm/carrageenan, especially for the salt with high concentrations.

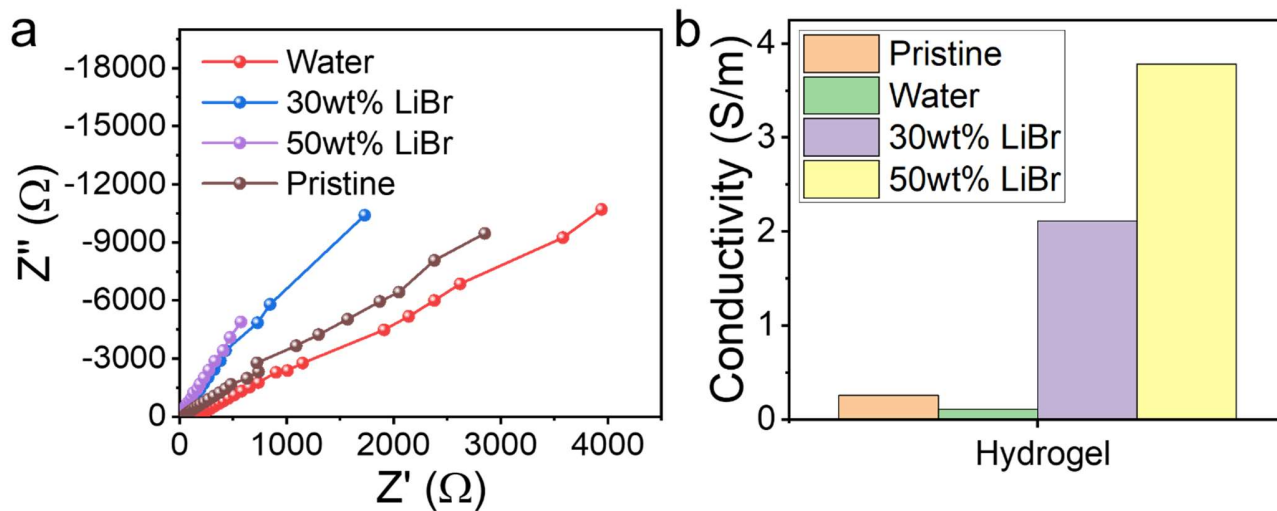


Figure S3. (a) Impedance spectra of hydrogels with different LiBr concentrations. (b) Conductivity of different hydrogels measured by the AC impedance method.

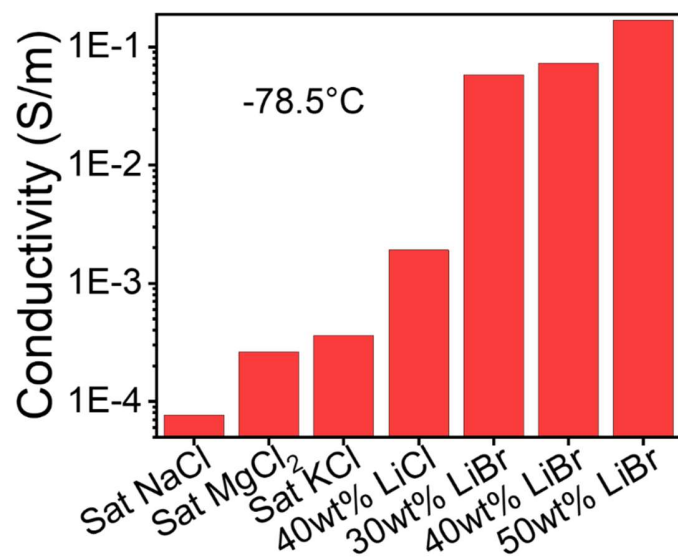


Figure S4. Conductivity of DN hydrogels at -78.5°C after immersion in saturated NaCl, saturated MgCl₂, saturated KCl, 40 wt% LiCl, 30 wt% LiBr, 40 wt% LiBr and 50 wt% LiBr aqueous solutions for 3 h.

Table S1. Conductivity of salt percolated hydrogels after immersion in different aqueous solution for 3h at -78.5°C.

Salt	Conductivity (S/m)
KCl	3.6×10^{-4}
NaCl	7.7×10^{-5}
MgCl ₂	2.6×10^{-4}
40 wt% LiCl	1.9×10^{-3}
30 wt% LiBr	5.7×10^{-2}
40 wt% LiBr	7.3×10^{-2}
50 wt% LiBr	1.7×10^{-1}

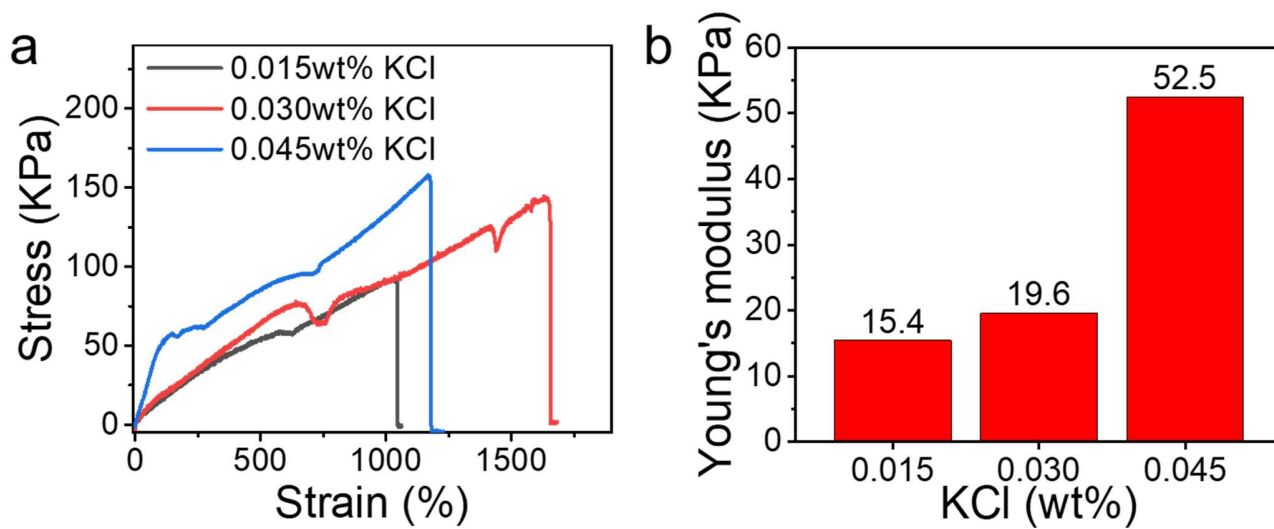


Figure S5. (a) Strain-stress curves of hydrogels with different KCl concentrations. (b) Comparison of Young's modulus of hydrogels with different KCl concentrations.

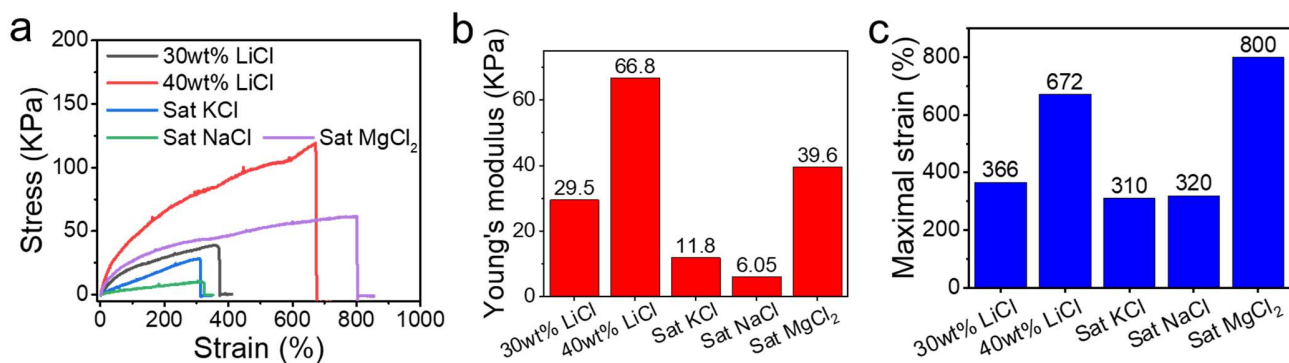


Figure S6. (a) Strain-stress curves, (b) comparison of Young's modulus, and (c) comparison of maximal tensile strain of hydrogels after immersion in saturated NaCl, saturated MgCl₂, saturated KCl, 30 wt% LiCl and, 40 wt% LiCl aqueous solutions for 3 h.

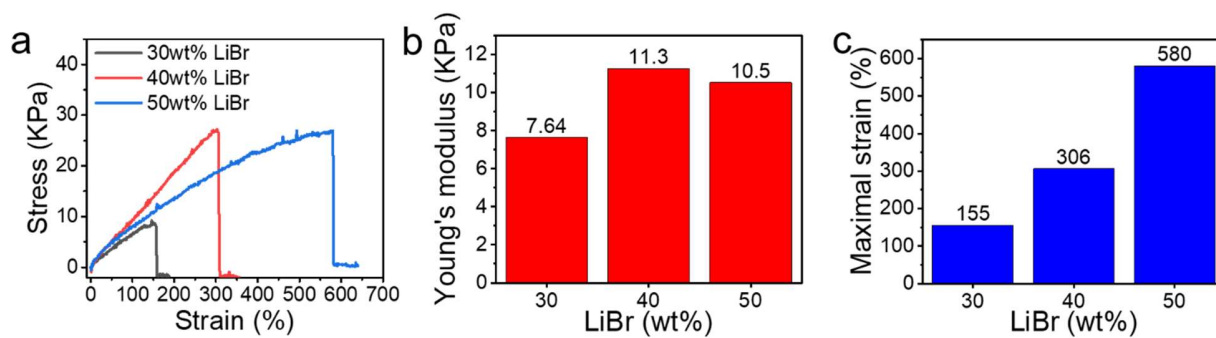


Figure S7. (a) Strain-stress curves, (b) comparison of Young's modulus, and (c) comparison of maximal tensile strain of hydrogels after immersion in 30 wt%, 40 wt% and 50 wt% LiBr aqueous solutions for 3 h.

Note 1. Calculation of the proportions of freezing and nonfreezing water in the hydrogel.

$$W_{\text{hydrogel}} = W_{\text{polymer}} + W_{\text{water}} + W_{\text{salt}}$$

$$W_{\text{freezing water}} = |\Delta H| / H_0 (\%)$$

$$W_{\text{nonfreezing water}} = W_{\text{water}} - W_{\text{freezing water}}$$

* H_0 is the specific enthalpy of fusion of pure water (334 J/g);¹ $|\Delta H|$ is the enthalpy of hydrogel freezing obtained by integration of the curve of DSC (Figure S8). For the pristine hydrogel, W_{water} is 82%. For the salt-percolated hydrogel, water is comprised of water in pristine hydrogel and the water adsorbed from salt aqueous water. The content of adsorbed water can be obtained from the swelling experiment (Figure 2b). Take 30wt% LiBr percolated hydrogel as an example:

$$W_{\text{water}} = [82 + (461-100) * (1-0.3)]/461 * 100 \% = 72.6\%$$

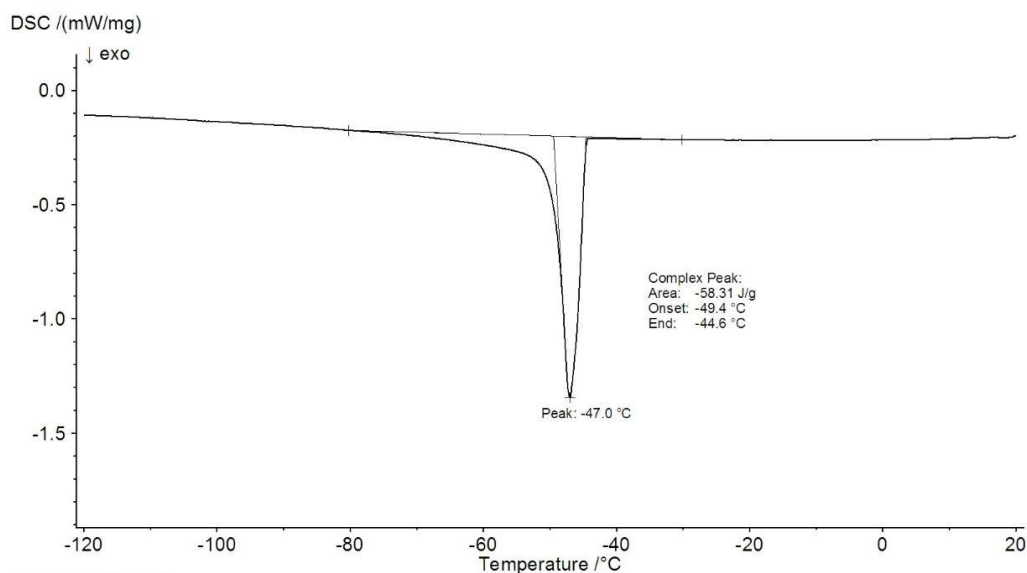


Figure S8. Integration of the DSC curve.

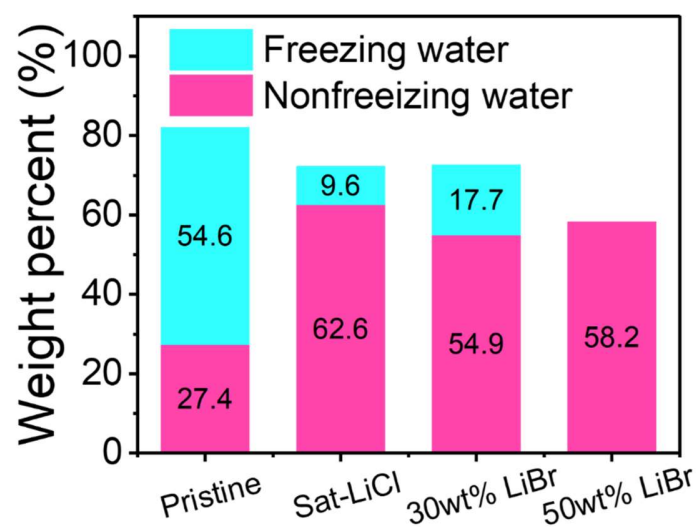


Figure S9. The weight percent of freezing and nonfreezing water in DN hydrogel before and after immersion in saturated LiCl, 30wt% and 50wt% LiBr aqueous solution.

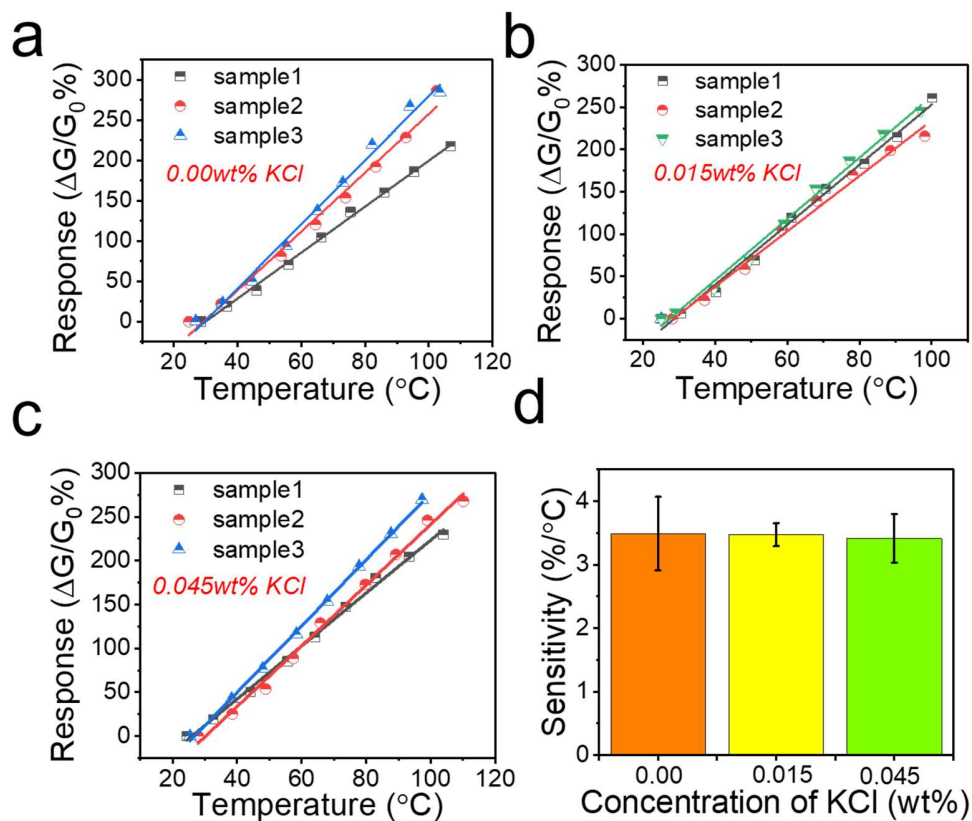


Figure S10. Linear fitting of thermal responses of hydrogels with different KCl concentrations: (a) 0.00wt%, (b) 0.015wt%, (c) 0.045wt%. (d) Thermal sensitivity versus KCl concentration. For each kind of KCl concentration, three samples were measured to obtain the average values.

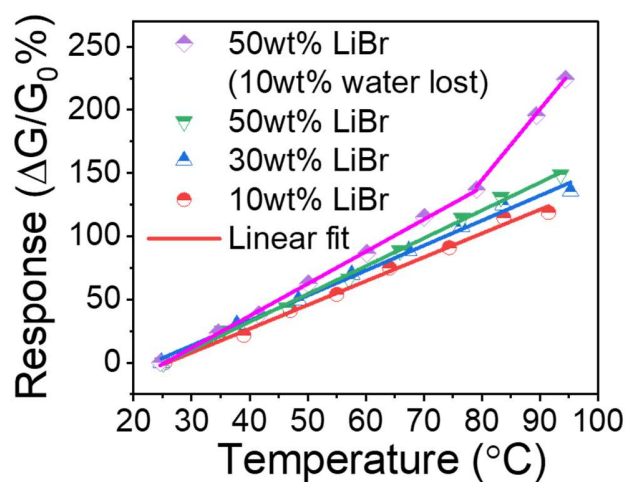


Figure S11. Linear fitting of responses of pristine, 10wt%, 30wt%, 50wt% LiBr hydrogels before and after partial dehydration (10wt% water lost) versus temperature curves.

Linearly fitted functions for the thermal responses of different hydrogels:

$$10\% \text{ LiBr: } y_2 = 1.88522x_2 - 48.62882$$

$$30\% \text{ LiBr: } y_3 = 1.97596x_3 - 45.69719$$

$$50\% \text{ LiBr: } y_4 = 2.20377x_4 - 55.88195$$

$$50\% \text{ LiBr (10\% water lost): } y_5 = 2.54045x_5 - 64.62643 (T \leq 79.1^\circ\text{C})$$

$$50\% \text{ LiBr (10\% water lost): } y_6 = 5.58204x_5 - 302.16387 (T \geq 79.1^\circ\text{C})$$

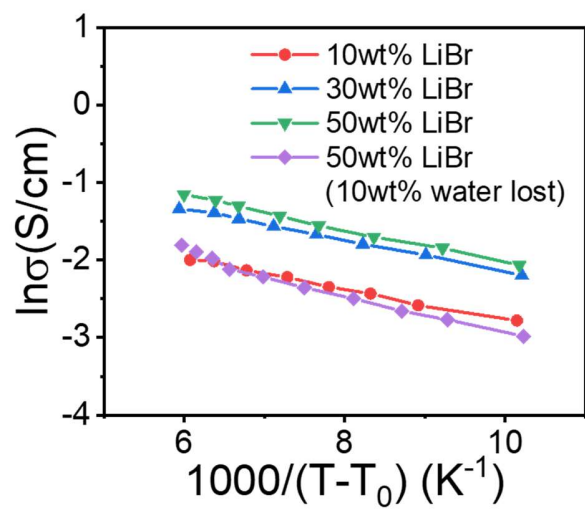


Figure S12. Vogel-Tammann-Fulcher (VTF) plots ($T_0=200K$) of the DN hydrogels with different LiBr concentrations.

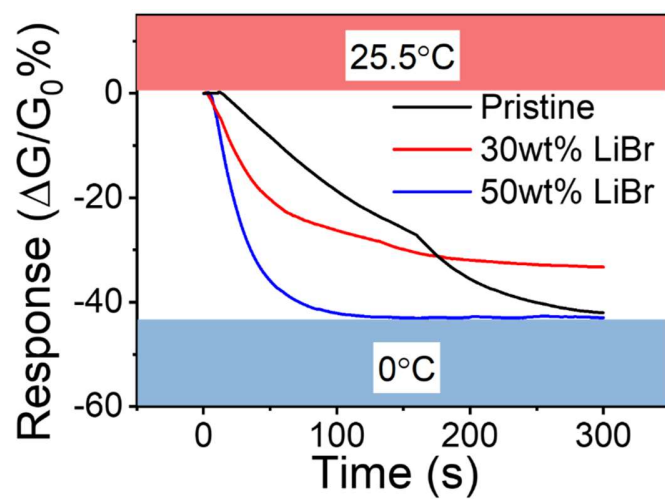


Figure S13. Dynamic responses of different hydrogels to the cooling from 25.5 to 0 °C, from which the response time of the sensors was analyzed, as shown in Figure 5e.

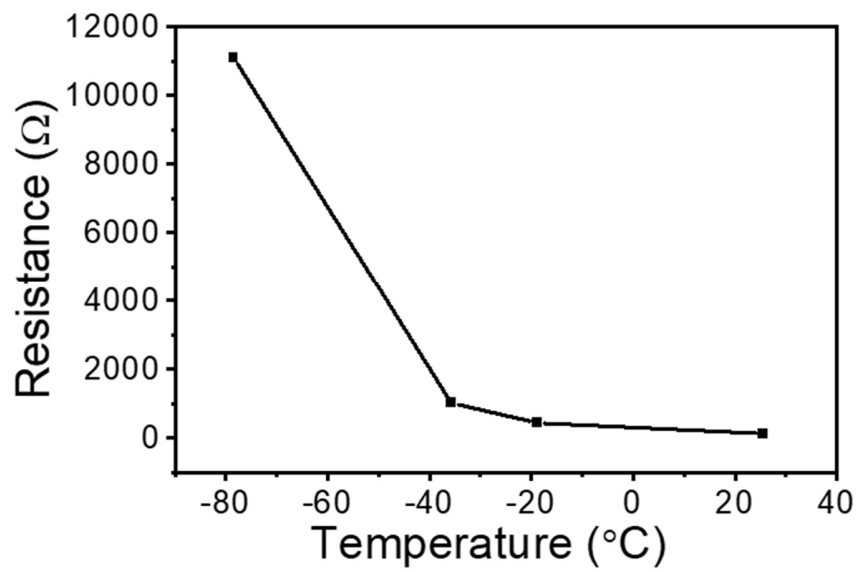


Figure S14. Plot of the resistance of 50wt% LiBr hydrogel versus temperature.

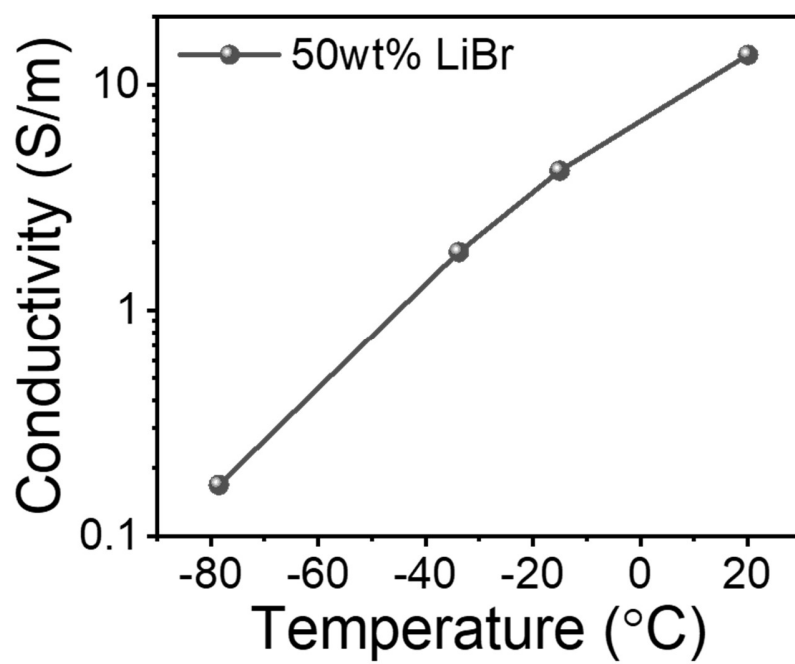


Figure S15. Plot of the conductivity of 50wt% LiBr hydrogel versus temperature.

Table S2. Comparison in the sensing properties of various stretchable temperature sensors reported recently.

Materials	Sensitivity(%/°C)	Detection range (°C)	Resistance/ conductivity (RT)	Transparent
PAA-PANI ²	1.64	40-110	~20 kΩ	No
(PAM)/MWCNTs/Fe ³⁺ - PAA ³	2.2	20-80	6.26 S/m	No
Cellulose/PVA ⁴	-0.03(TCR)	-12.4-60	0.46 S/m	Yes
oligo(ethylene glycol) methacrylate ⁵	/	-20-45	0.0332 S/m	Yes
LiBr-PAM/carrageenan this work	2.54	-78.5-97	12 S/m	Yes

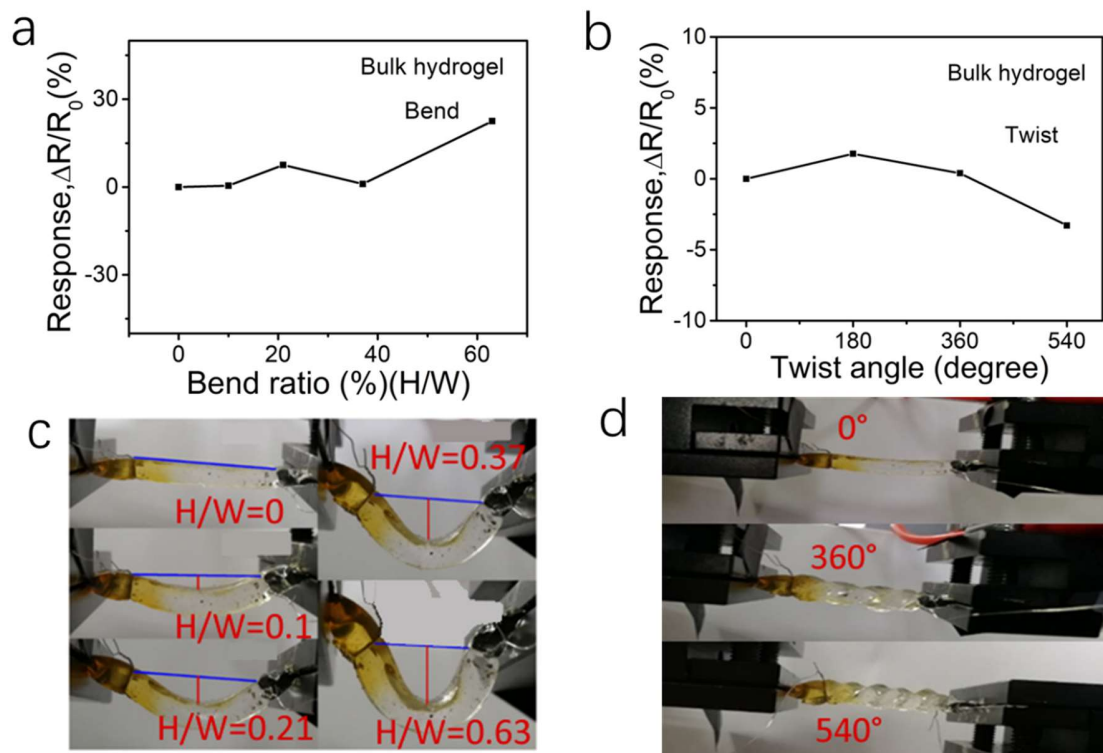


Figure S16. Responses of the hydrogel to flexion and twist deformations. a) and b) Dynamic responses to varying bend ratio and twist angle, respectively. The bend ratio is defined as the ratio of height to width. c-d) Photographs showing the hydrogel under different bend ratios and twist angles.

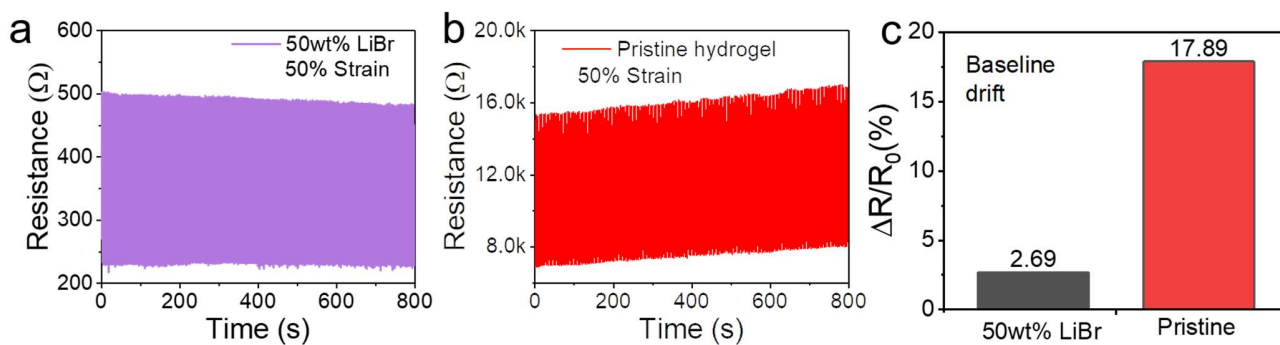


Figure S17. (a-b) Cyclical resistance variations of 50wt% LiBr and pristine hydrogels versus time in the detection of 50% strain for 180 successive cycles. (c) Comparison in the baseline drifts ($\Delta R/R_0$ %) of 50wt% LiBr and pristine hydrogels after successive loading and unloading of 50% stain for 180 cycles.

REFERENCES

1. W. Ge, S. Cao, Y. Yang, O. J. Rojas and X. Wang, *Chem. Eng. J.*, 2021, **408**, 127306.
2. G. Ge, Y. Lu, X. Qu, W. Zhao, Y. Ren, W. Wang, Q. Wang, W. Huang and X. Dong, *ACS Nano*, 2020, **14**, 218-228.
3. R. An, X. Zhang, L. Han, X. Wang, Y. Zhang, L. Shi and R. Ran, *Sci. Eng. C*, 2020, **107**, 110310.
4. Y. Wang, L. Zhang and A. Lu, *J. Mater. Chem. A*, 2020, **8**, 13935-13941.
5. P. Wei, T. Chen, G. Chen, H. Liu, I. T. Mugaanire, K. Hou and M. Zhu, *ACS Appl. Mater. Interfaces*, 2020, **12**, 3068-3079.